JGR Oceans

RESEARCH ARTICLE
10.1029/2021JC017486

Regionalization of the Red Sea Based on Phytoplankton Phenology: A Satellite Analysis

Malika Kheireddine[1], **N. Mayot**[2], **M. Ouhssain**[1], **and B. H. Jones**[1]

[1]Red Sea Research Center (RSRC), Biological and Environmental Sciences and Engineering Division (BESE), King Abdullah University of Science and Technology (KAUST), Thuwal, Saudi Arabia, [2]School of Environmental Sciences, Faculty of Science, University of East Anglia, Norwich, UK

Key Points:

- Bio-regionalization reveals four distinct regions that present different phytoplankton phenology in the Red Sea
- Fall-winter mixing events in the northern area and the monsoon-driven winds in the southern area explain the four phytoplankton phenologies
- Inter-annual variability in phytoplankton phenology in response to variations in air-sea heat fluxes or El Niño Southern Oscillation phases

Supporting Information:

Supporting Information may be found in the online version of this article.

Correspondence to:

M. Kheireddine,
Malika.kheireddine@kaust.edu.sa

Citation:

Kheireddine, M., Mayot, N., Ouhssain, M., & Jones, B. H. (2021). Regionalization of the Red Sea based on phytoplankton phenology: A satellite analysis. *Journal of Geophysical Research: Oceans*, *126*, e2021JC017486. https://doi.org/10.1029/2021JC017486

Received 19 APR 2021
Accepted 27 SEP 2021

Abstract The current average state of Red Sea phytoplankton phenology needs to be resolved in order to study future variations that could be induced by climate change. Moreover, a regionalization of the Red Sea could help to identify areas of interest and guide *in situ* sampling strategies. Here, a clustering method used 21 years of satellite surface chlorophyll-a concentration observations to characterize similar regions of the Red Sea. Four relevant phytoplankton spatiotemporal patterns (i.e., bio-regions) were found and linked to biophysical interactions occurring in their respective areas. Two of them, located in the northern part the Red Sea, were characterized by a distinct winter-time phytoplankton bloom induced by mixing events or associated with a convergence zone. The other two, located in the southern regions, were characterized by phytoplankton blooms in summer and winter which might be under the influence of water advected into the Red Sea from the Gulf of Aden in response to the seasonal monsoon winds. Some observed inter-annual variabilities in these bio-regions suggested that physical mechanisms could be highly variable in response to variations in air-sea heat fluxes and ENSO phases in the northern and southern half of the Red Sea, respectively. This study reveals the importance of sustaining in situ measurements in the Red Sea to build a full understanding about the physical processes that contribute to phytoplankton production in this basin.

Plain Language Summary The Red Sea has been characterized as an area sensitive to climate change, which may affect the Red Sea phytoplankton phenology. A better understanding on the factors controlling the phytoplankton phenology is needed. We thus performed a regionalization of the Red Sea using 21 years of satellite surface chlorophyll-a concentration observations to characterize similar regions of the Red Sea. We identified four relevant phytoplankton spatiotemporal patterns named "bio-regions" linked to the physical characteristics within each region. The northern Red Sea bio-regions are marked by a winter phytoplankton bloom due to mixing events that may uplift nutrients towards the surface layer. The southern Red Sea bio-regions, marked by summer and winter phytoplankton blooms, are mainly related to the summer southwest monsoon as well as the winter northeast monsoon, which favors the intrusion of sub-surface and surface nutrient-rich waters from the Gulf of Aden, respectively. These findings provide a better understanding of phytoplankton phenology in the Red Sea while in situ measurements are still needed for a full comprehension of the processes that contribute to phytoplankton seasonal cycle in the basin. Such comprehension is of fundamental interest for identifying and explaining ongoing changes and predicting future changes in Red Sea biological.

1. Introduction

The Red Sea is a marine biodiversity hotspot, surrounded by coral reefs and mangroves, which favors the development of specific ecological niches (Baars et al., 1998). Phytoplankton organisms in this basin, as in the rest of the global ocean, play a key role in pelagic marine ecosystem's functioning. Moreover, phytoplankton cells influence the production and vertical export of organic carbon, a key component of the carbon cycle that impacts the atmospheric concentration of CO_2 (Bopp and Le Quéré, 2009; Boyd et al., 2019; Kheireddine et al., 2020). Recent studies showed that the Red Sea is a rapidly warming region of the global ocean (Chaidez et al., 2017). Such important environmental change may strongly affect the dynamic of the phytoplankton, especially its phenology (i.e., timing and intensity of phytoplankton growth) which, in turn could affect marine food webs as well as the efficiency of the biological carbon pump (Cushing, 1990; Koeller et al., 2009; Platt et al., 2003). Indeed, changes in phytoplankton phenology may induce, for example,

potential mismatch between primary producers, grazers and apex predators (Ardyna et al., 2014; Edwards & Richardson, 2004), which impacts the vertical export of organic carbon aggregates to the deep ocean (Dall'Olmo et al., 2016). Because the Red Sea is a small and semi-enclosed basin, those modifications might be accelerated and could rapidly impact the whole ecosystem compared to other oceanic regions (Kheireddine et al., 2020).

Since the last decade, there has been a growing interest toward understanding phytoplankton dynamics (i.e., occurrence, timing and intensity of blooms) throughout the global ocean (Behrenfeld & Boss, 2018; Boyce et al., 2017; Sathyendranath et al., 2015). The Red Sea can be considered as a natural laboratory to study the role of the phytoplankton phenology in the context of climate change, because this oceanic basin includes conditions which may occur in diverse tropical areas of the global ocean. A first step is to describe the current average state of the phytoplankton phenology in the Red Sea before evaluating any changes that might be linked to natural mechanisms or in response to climate variability. Moreover, at a basin scale, studying the phytoplankton phenology and its spatial variability could be used to assess the primary environmental processes affecting the phytoplankton production and thereby some of the ecosystem's functioning (Edwards & Richardson, 2004).

Few studies have attempted to study the phytoplankton phenology in the Red Sea (Asfahani et al., 2020; Dreano et al., 2016; Gittings, Brewin, et al., 2019; Labiosa et al., 2003; Lindel & Post, 1995; Raitsos et al., 2013). Most of these studies focused on sub-regions of the Red Sea or were based on limited in situ data. Recently, Gittings, Raitsos et al. (2019) studied the phytoplankton phenology based on in situ data in the northern Red Sea (above 25°N) and showed that ocean color remote sensing is a powerful tool to assess the overall water column dynamics and the phytoplankton phenology.

Using ocean color remote sensing observations of chlorophyll-a concentration (CHL), a proxy of phytoplankton biomass, Raitsos et al. (2013) attempted to characterize the Red Sea phytoplankton phenology. They proposed to divide the Red Sea into regions, based on latitude bands, and to associate them with four annual cycles of phytoplankton biomass. However, there was an absence of statistical confirmation about the relevance and locations of the four regions proposed. The four seasonal cycles were obtained using a climatological approach without considering the inter-annual variability. Finally, their study focused only on the absolute values of CHL rather than the relative differences in phytoplankton biomass between seasons. Therefore, their proposed regionalization of the Red Sea needs to be refined with a more comprehensive statistical clustering analysis of satellite CHL data.

In this study, we reinvestigated ocean color remote sensing dataset of CHL in the Red Sea, in order to provide information on phytoplankton phenology (timing, duration and intensity of the bloom) in different areas of the basin based on a method developed by D'Ortenzio and d'Alcala (2009) and by considering potential inter-annual variability. This method has proven its efficiency and has been previously applied in diverse oceanic areas (i.e., Mediterranean Sea, North Atlantic Ocean, Southern Ocean) (Ardyna et al., 2017; D'Ortenzio and d'Alcala 2009; Lacour et al., 2015; Mayot et al., 2016) and at global scale (D'Ortenzio et al., 2012). The main goals here are to (a) identify bio-regions based on observed annual cycles of phytoplankton biomass and (b) to suggest mechanisms driving the phytoplankton dynamic and its inter-annual variability. Such information will improve the comprehension of Red Sea ecosystem's functioning, as well as the potential impact of climate change on this oceanic basin.

2. Material and Methods

2.1. Clustering Satellite Estimates of Chlorophyll-a Concentration

Ocean color measurements of CHL were retrieved from the version 4.2 of the European Space Agency's Ocean Colour Climate Change Initiative (OC-CCI) Level-3 data product (http://www.esa-oceancolour-cci.org) (Sathyendranath et al., 2019, 2020). The OC-CCI product refers to merged and bias-corrected measurements acquired from the Moderate Resolution Imaging Spectroradiometer on the Aqua Earth Observing System (MODIS-Aqua), the Sea-viewing Wide Field-of-view Sensor (SeaWiFS), the Medium Resolution Imaging Spectrometer (MERIS) and the Visible Infrared Imaging Radiometer Suite (VIIRS) satellite sensors. Satellite images were extracted for the period 1998–2018, and had spatial and temporal resolutions of 4 km

and 8 days, respectively. Note that, the OC-CCI data used in this study has been developed, validated, and distributed by Plymouth Marine Laboratory, UK.

Firstly, a regionalization of the Red Sea basin was performed by using 8-day climatological satellite composite images of CHL and by applying a methodology similar to D'Ortenzio and d'Alcala (2009). This analysis regrouped pixels having similar CHL annual cycle (i.e., phytoplankton phenology) into clusters (i.e., bio-regions), which defined distinct bio-regions. Such an analysis focuses on the general shape of the annual cycle by filtering out non-significant day-to-day variations as recommended by Racault et al. (2012, 2014). In more detail, climatological annual cycles of CHL were obtained by averaging at each pixel location the CHL measured the same 8-day period (i.e., 1–8 January, 9–16 January, etc.). Temporal gaps in obtained climatological time series were filled by applying a linear interpolation method. However, time series with temporal gaps larger than a month or with half of the data missing were discarded. All estimated climatological annual cycles were divided by their annual maximum values. This climatological dataset of normalized CHL annual cycles was clusterized with a fuzzy c-means, where the number of cluster (C) was set to four based on a silhouette analysis (Supporting Information S1). Obtained clustering results included four cluster centers and a map with the location of the time series belonging to each cluster. A cluster center was defined as the mean of all CHL annual cycles belonging to a cluster. Some phytoplankton phenology metrics were retrieved from these four cluster centers: bloom initiation, termination and duration, as well as its maximum intensity using the threshold criterion method (Gittings et al., 2018; Gittings, Raitsos, et al., 2019; Racault et al., 2012).

Secondly, yearly datasets of normalized CHL annual cycles were clusterized. In practice, at each pixel location the 21 years long time series of CHL was divided into yearly time series from July of year n-1 to late June of year n, and temporal gaps where filled with a linear interpolation. Each yearly annual cycle of CHL was normalized by its maximum value. Annual cycles with temporal gaps larger than a month or with more than half of data missing were discarded. Each of 21 yearly datasets was clusterized with a fuzzy c-means with the cluster centers from the climatological clustering results (see above) used as guesses. However, the number of available CHL annual cycles (without temporal gaps) in the south of the Red Sea was low. Therefore, this yearly clustering of the Red Sea was only performed in the north of the Red Sea with the two clusters centers mostly observed in this area (see Section 3 and Supporting Information S1). All R scripts used to perform these clustering analyses are publicly available on GitHub (https://github.com/nmayot/RedSea_regionalization).

2.2. Auxiliary Datasets: Mixed Layer Depth (MLD) and El Nino Index

The Mixed Layer Depth (MLD) data from the Mercator model (GLOBAL_REANALYSIS GLORYS12V1 product), were downloaded through the Copernicus Marine Environment Monitoring Service (CMEMS) Web Portal Subsetter Service. Monthly data fields on a standard regular grid at 1/12° (~8 km) were used. The MLD was defined as the depth at which temperature exceeded the temperature at 10 m by 0.2°C (de Boyer Montégut et al., 2004). The quality information document for the Global Ocean Reanalysis products can be found at https://resources.marine.copernicus.eu/documents/PUM/CMEMS-GLO-PUM-001-030.pdf.

Monthly values of the multivariate El Niño Southern Oscillation (ENSO) Index (MEI) were downloaded from the National Oceanic and Atmospheric Administration (NOAA) (http://www.esrl.noaa.gov/psd/enso/mei/). The computational details of the index can be found in Wolter and Timlin (1993, 1998).

3. Results and Discussion

3.1. Red Sea Bio-Regions

The climatological clustering method identified four distinct bio-regions in the Red Sea (Figure 1, Table 1) corresponding to different bloom phenologies. The existence of those bio-regions suggests that the Red Sea is characterized by a high variability in annual cycle of phytoplankton biomass. Moreover, the bio-regions were distributed along a latitudinal gradient with, sometimes, the coexistence of several bio-regions at the

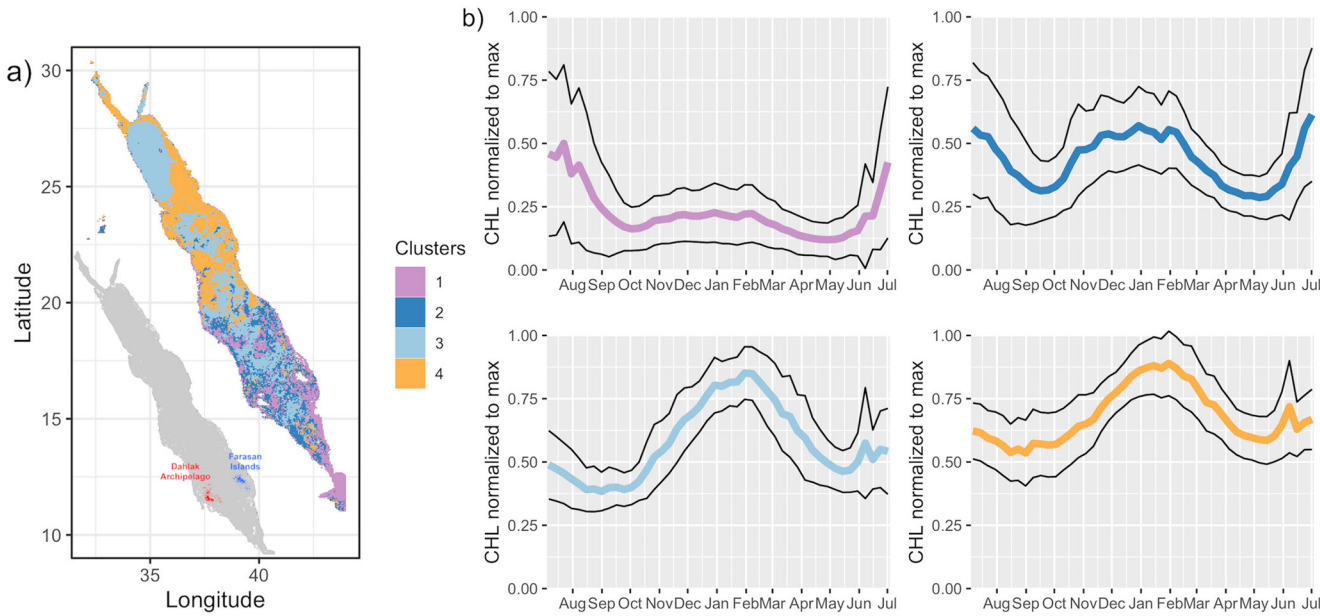

Figure 1. Regionalization of the phytoplankton phenology in the Red Sea. (a) Spatial distribution of the four bio-regions obtained with a fuzzy c-means clustering method applied to a dataset of climatological annual cycles of normalized CHL. (b) Annual cycle of normalized CHL of each bio-region. Thick lines depict averages and thin lines indicate the 1σ intervals.

same latitude (Figure 1). Such spatial distribution suggests that phytoplankton dynamics might be related to the basin circulation dynamic and/or the availability in nutrients (Eladawy et al., 2017; Gittings et al., 2018; Papadopoulos et al., 2013, 2015; Racault et al., 2015; Raitsos et al., 2013; Zarokanellos and Jones, 2021).

Table 1
Main Characteristics of Each Bio-Region Presented in Figure 1

Characteristics	Bio-region 1	Bio-region 2	Bio-region 3	Bio-region 4
Spatial distribution	Southern Red Sea	Southern Red Sea	Northern Red Sea	Northern Red Sea
	Around the Farasan islands and the Dahlak Archipelago		The extreme northern Red Sea and the Gulf of Aqaba	The north central Red Sea, The Northwestern coast and the Gulf of Suez
Phytoplankton bloom	Summer bloom (July–August)	Summer & Fall-Winter blooms (July) (November–February)	Winter bloom (November–February)	No winter bloom? (November–February)
	(Racault et al., 2015)	(Racault et al., 2015)	(Kheireddine et al., 2020)	(Zarokanellos and Jones, 2021)
Seasonality (mg m^{-3})	Median (Min. to Max.)	Median (Min. to Max.)	Median (Min. to Max.)	Median (Min. to Max.)
	3.5 (0.36 to 13.07)	0.96 (0.2 to 4.05)	0.19 (0.12 to 0.50)	0.13 (0.06 to 0.25)
Annual CHL (mg m^{-3})	0.65 (0.02 to 2.23)	0.57 (0.005 to 2.1)	0.19 (0.004 to 0.51)	0.18 (0.06 to 0.44)
Annual MLD (m)	11 (8 to 16)	15 (7 to 22)	34 (11 to 71)	25 (11 to 50)
Source of nutrients	Southwest monsoon (Intrusion of sub-surface nutrient-rich waters from the Gulf of Aden) (Churchill et al., 2014)	Southwest & Northeast Monsoons (Intrusion of sub-surface & surface nutrient-rich waters from the Gulf of Aden) (Churchill et al., 2014)	Mixing events supplying nutrients in the surface layer (Kheireddine et al., 2020 and references therein)	No nutrients (Dispersion of the subsurface chlorophyll maximum) (Zarokanellos and Jones, 2021)
Dominant Phytoplankton functional types	Winter/Spring/Summer/Fall			
	Micro-/Nano-/Micro/Micro-phytoplankton (Brewin et al., 2015)		Micro-/Nano-/Pico/Pico-phytoplankton (Brewin et al., 2015)	

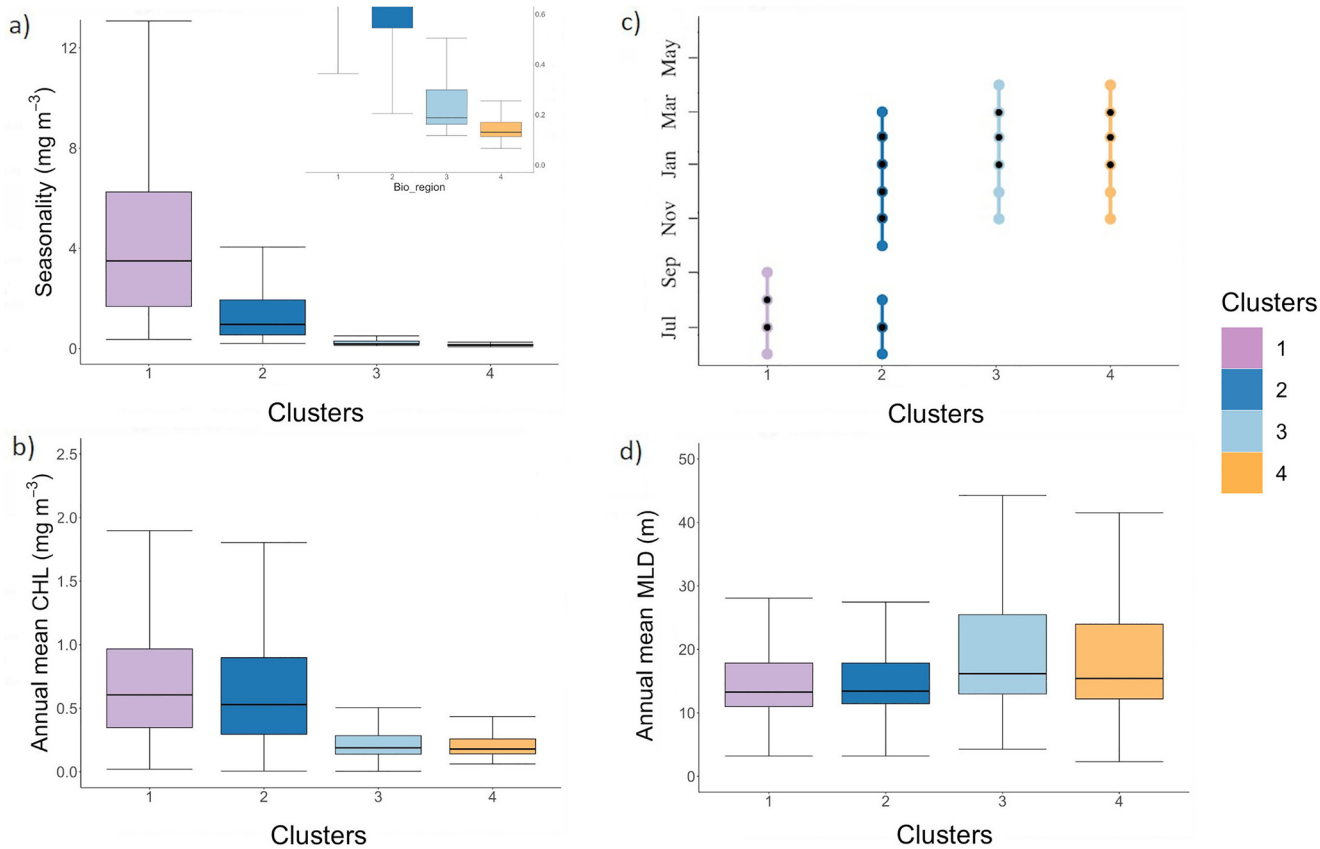

Figure 2. The chlorophyll-a seasonality (i.e., amplitude) (mg m^{-3}) associated to a zoom on Bio-regions 3 and 4 (a), the annual mean chlorophyll-a concentration (mg m^{-3}), the timing of the bloom maximum where the black dots correspond to the most frequent month where we observed the highest bloom intensity (month; *y* axis) (c) and annual mean MLD (d).

Moreover, the phytoplankton phenology (i.e., timing and intensity of phytoplankton bloom) was significantly different between these bio-regions (Figure 2).

In the northern half (above 20°N) of the Red Sea basin, Bio-regions 3 and 4 were mostly observed. The annual cycle associated with Bio-region 3 was characterized by a phytoplankton bloom that initiated in November, terminated in mid-April and had a mean duration of about 5 months. The annual maximum value of CHL was generally observed between January and February (Figure 2c). In the Bio-region 4, the annual cycle of CHL was also characterized by a winter phytoplankton bloom that initiated in mid-November, reached its maximum value between mid-December and mid-March and terminated in mid-April (Figure 2c). However, the winter phytoplankton bloom intensity was lower in Bio-region 4 than in Bio-region 3 (Figure 2a). Actually, within the Red Sea, it was the Bio-region 4 that exhibited the lowest CHL values (Figure 2b). Such differences between Bio-regions 3 and 4 might be due to variations in air-sea heat fluxes and the physical dynamic of the basin (Dasari et al., 2018; Gittings et al., 2018; Papadopoulos et al., 2013, 2015) (Figure 2a).

In fact, in winter (from October to March) in the northern half of the Red Sea, there are distinct physical mechanisms between these two bio-regions. The phytoplankton seasonal cycle observed in Bio-region 3 seems to be related to vertical mixing occurring in winter (Figures 2d and 3) that supply cold-nutrient-rich waters within the surface layer (Asfahani et al., 2020; Gittings et al., 2018, Gittings, Raitsos et al., 2019; Kheireddine et al., 2020; Torfstein & Kienast, 2018; Triantafyllou et al., 2014). While in the Bio-region 4, the phytoplankton bloom might be sustained by the surface circulation of the basin associated with the winds (Langodan et al., 2014; Morcos, 1970). In winter, a northwesterly wind blows over the northern half of the basin whereas the southern half of the basin (below 20°N) is dominated by a southeasterly wind. The collision of the northwest and southeast winds occurs around 18°–25°N (Figures S3_1, S3_2 and S3_3

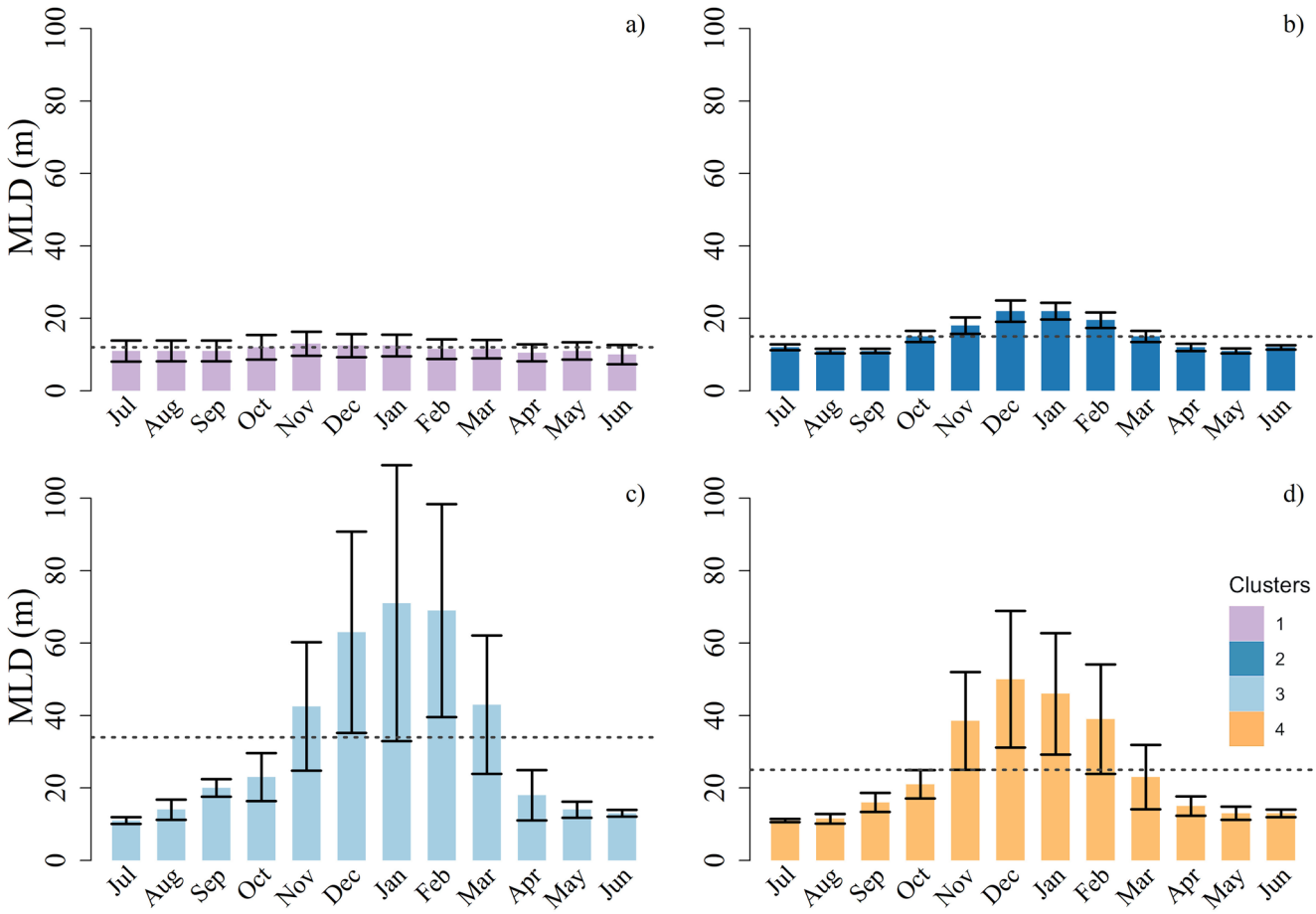

Figure 3. For each bio-region, average ± standard deviation of the annual cycles of the mixed layer depth (MLD). The dashed dark gray line represent the yearly average value of the MLD.

in Supporting Information S1, Dasari et al., 2018; Langodan et al., 2014; Morcos, 1970) and can lead to a convergence zone where nutrients are supplied within the surface layer favoring the initiation of the phytoplankton bloom observed in November in the Bio-region 4 (Figure 1). Recently, Zarokanellos and Jones (2021) showed that mixing events dispersed phytoplankton from the deep CHL maximum (DCM) increasing near-surface CHL in this region. This suggests that the Bio-region 4 could simply correspond to the redistribution of the phytoplankton biomass vertically in response to mixing events. Indeed, the Bio-region 4 seems to not be marked by a sufficient deepening of the MLD to uplift nutrients toward the surface layer (Figure 3).

Bio-region 3 and 4 were also characterized by a recurrent summer peak in CHL in June, which is consistent with the findings of Raitsos et al. (2013). Raitsos et al. (2013) suggested that this summer CHL peak is due to the apparent presence of anti-cyclonic mesoscale eddies, lasting for 2 to 3 weeks in June in this region. These mesoscale eddies can occupy large areas of the northern half of the basin and are generally surrounded by coastal coral reefs (Figure S4 in Supporting Information S1) (Acker et al., 2008; Raitsos et al., 2013), which can thus supply nutrients and/or phytoplankton biomass (through advection) within the surface layers (Kheireddine et al., 2017, 2018).

In the southern half of the Red Sea, the spatial distribution of the bio-regions was highly variable with three bio-regions (Bio-regions 1, 2 and 3) identified. While Bio-region 3 was detected in this southern part of the basin, the core of this bio-region was located in the northern part of the Red Sea (Figure 4) and its occurrence in the southern areas might be related to mesoscale features (Figures 4 and S4 in Supporting Information S1) (Zhan et al., 2014, 2018). Indeed, when looking at the probability of membership of all

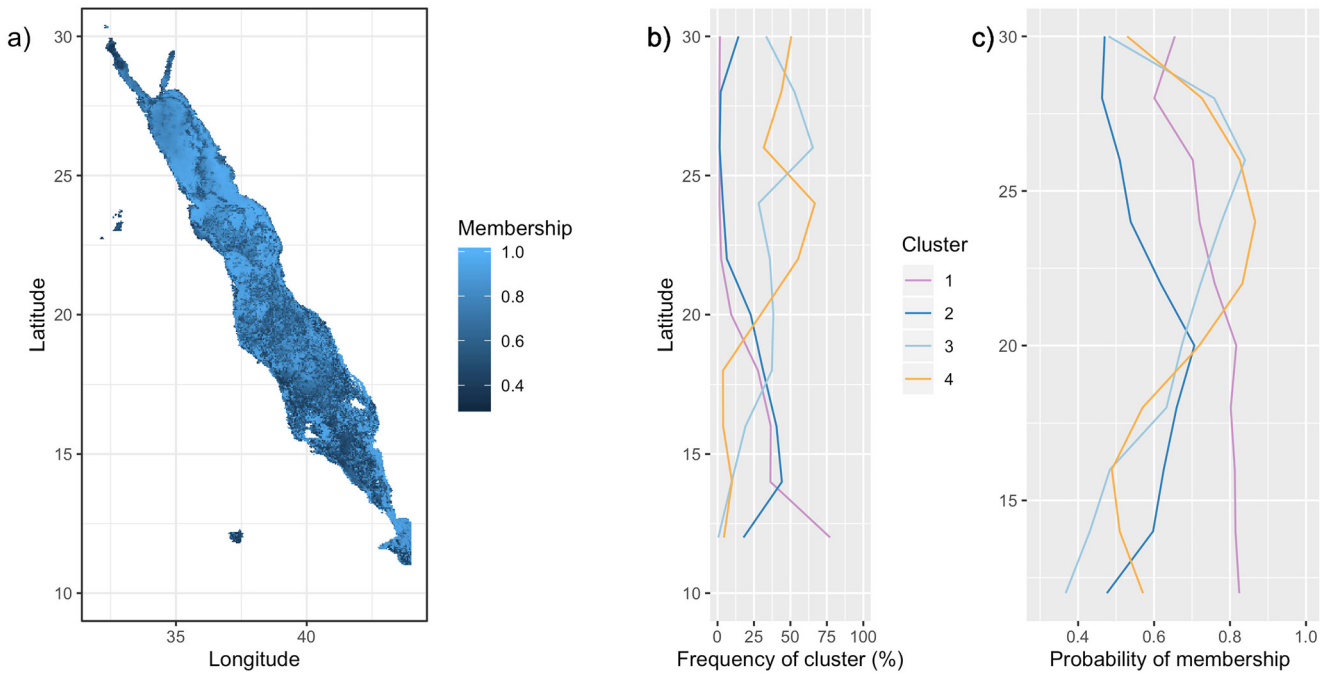

Figure 4. Probability of bio-region membership. (a) Probabilities of membership of each pixel to its assigned bio-region. Trend lines on the right depict (b) the frequency of occurrence of each bio-region by latitude, and (c) the average probability of membership by latitude for each bio-region. Latitudinal bands of 2° were used.

pixels associated with Bio-region 3 along the latitudes (Figure 4c), those values decreased towards the south. This confirmed that annual cycles associated with the Bio-region 3 in the northern part of the Red Sea were closer to the cluster center than the ones located in the southern part.

The Bio-region 1 was characterized by a summer phytoplankton bloom which initiated at the end of May, peaked in July and collapsed through August to terminated in September (Figures 1 and 2c). This bio-region mainly occupied the southeastern shore around the Farasan islands and also the Dahlak Archipelago (Figures 1 and 4) corresponding to shallow reef-bound coastal waters (Genevier et al., 2019; Racault et al., 2015). Such seasonal variability might be due to the summer southwest monsoon, which favors the intrusion of sub-surface nutrient-rich waters from the Gulf of Aden Intermediate Water (GAIW) along the shallow coral reefs area (Churchill et al., 2014; Dreano et al., 2016; Racault et al., 2015). The bio-region 2 was characterized by a peak in CHL in summer (initiated at the end of May and terminated in September) and in fall-winter (October to February) (Figure 2c) which might be the consequences of the summer southwest monsoon and the winter northeast monsoon, respectively. Indeed, the winter northeast monsoon favors the horizontal advection of cold nutrient-rich surface waters from the Gulf of Aden mainly along the southwestern shore whereas the summer southwest monsoon favors a subsurface intrusion of cool nutrient-rich intermediate water from the Gulf of Aden in coral reefs complex along the south basin's shore (below 20°N) (Churchill et al., 2014; Yao, Hoteit, Pratt, Bower, Kohl, et al., 2014; Yao, Hoteit, Pratt, Bower, Zhai et al., 2014). This agreed with previous studies that showed that the southern Red Sea productivity and phytoplankton phenology is mainly influenced by the monsoon-driven winds (Acker et al., 2008; Dreano et al., 2016; Raitsos et al., 2013, 2015; Racault et al., 2015) and not due to variations in the MLD (Figure 3). Finally, onshore coastal habitats and shallow waters of the southern Red Sea were marked by higher CHL values than in the northern bio-regions (Figures 2a, 2b and 5). This suggests that the northern half is more oligotrophic than the southern half. This is coherent given that the Red Sea is considered oligo- to meso-trophic in nature (Raitsos et al., 2013). Indeed, the northern Red Sea is the most oligotrophic associated to small phytoplankton cells size (pico-phytoplankton) except during the bloom period (i.e., Fall-Winter seasons) where large phytoplankton cells (nano-phytoplankton) predominate (Table 1, Brewin et al., 2015). Conversely, the southern bio-regions and around coral reef-bound coastal waters are only associated to large phytoplankton cells (micro- and nano-phytoplankton) all year (Table 1, Brewin et al., 2015).

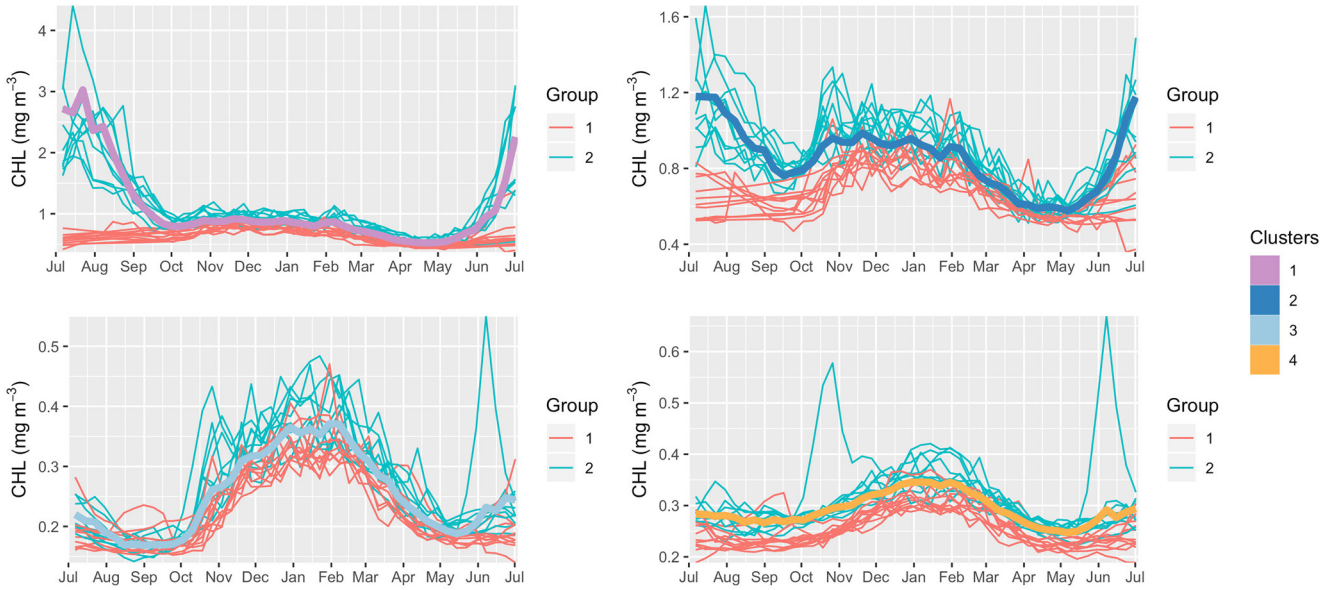

Figure 5. Climatological annual cycles vs. yearly annual cycles. For each bio-region, the climatological annual cycles chlorophyll-a concentration (thick lines) is compared with all 21 annual cycles available (thin lines, from 1998 to 2018). The two group of years mentioned in "Inter-annual variability in annual cycle of CHL" within the manuscript and Table 1 are highlighted, Group 1: 1998 to 2001 and 2012 to 2018; Group 2: 2002 to 2011.

3.2. Inter-Annual Variability in Annual Cycle of CHL

When looking at all the yearly annual cycles (21 cycles), annual cycles of CHL were more variable in Bio-regions 1 and 2 than in Bio-regions 3 and 4 (Figure 5). Indeed, there were two distinct groups of years (Figure 5, Table 2) that had different CHL annual cycles in Bio-regions 1 and 2, while only small variations in annual cycles of CHL can be observed in the northern half of the Red Sea (Bio-regions 3 and 4). Such differences between the northern and southern areas of the Red Sea could be due to the lower availability of yearly CHL annual cycle in the southern part of Red Sea (Figure S2 in Supporting Information S1). However, the lower coverage of satellite data might not be the only reason for these differences. Indeed, group of years 1 and 2 seemed to be related to negative and positive ENSO phases, respectively (Table 2).

Previous studies showed that the ENSO can influence the global climate on seasonal to inter-annual time scales (Wolter & Timlin, 2011) and affect the phytoplankton phenology in the global ocean (Behrenfeld et al., 2006; Chavez et al., 2011) and in the Red Sea (Gittings et al., 2018; Raitsos et al., 2015).

During positive ENSO phases, which are associated to a warmer global climate (Reid & Beaugrand, 2012; Wolter & Timlin, 2011), previous studies observed an increase in stratification, a deeper nutricline and thus a reduced CHL concentrations in the ocean, particularly in tropical ecosystems (Martinez et al., 2009; Reid & Beaugrand, 2012; Racault, Sathyendranath, Brewin, et al., 2017; Racault, Sathyendranath, Menon, et al., 2017). In the Red Sea, Raitsos et al. (2015) showed that during positive (negative) ENSO phases, the advection of nutrients from the Gulf of Aden into the southern part of the basin is intensified (reduced); which could explain the observed changes in phytoplankton phenology in the southern part of the Red Sea (i.e., Bio-regions 1 and 2). In contrast, the phytoplankton phenology in the northern bio-regions (above 25°N) seemed to be less influenced by ENSO phase variations, as suggested by Gittings et al. (2018). This is consistent with the findings of Karnauskas and Jones (2018) where they showed that ENSO drives sea

Table 2
Years and MEI Phase Associated to Group 1 and Group 2 Highlighted in Figure 5

	Group 1	Group 2
Years	1998, 1999, 2000, 2001, 2012, 2013, 2014, 2015, 2016, 2017, 2018	2002, 2003, 2004, 2005, 2006, 2007, 2008, 2009, 2010, 2011
MEI phase	Mainly negative (72%)	Mainly positive (85%)

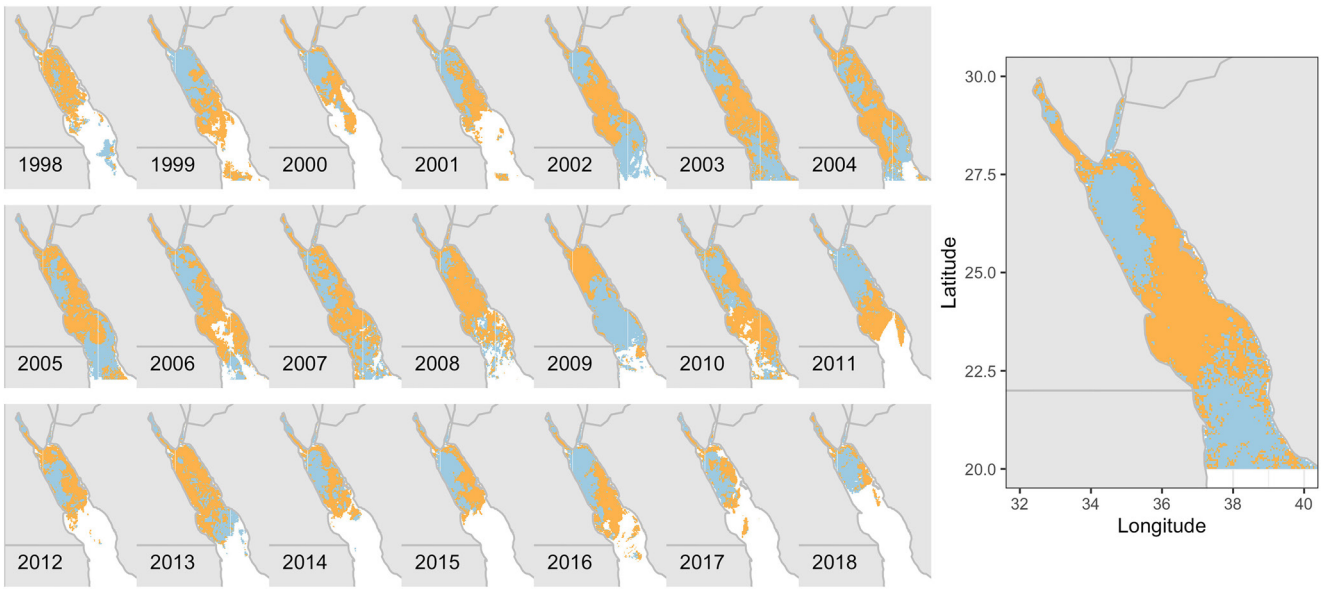

Figure 6. Annual clustering results from the northern part of the Red Sea. (left) Annual spatial distribution of bio-regions #3 and #4 from 1998 to 2018, and (right) the average map.

surface temperature anomalies in the southern Red Sea whereas the North Atlantic Oscillation drives those in the northern Red Sea.

However, spatial variations in phytoplankton phenology was not considered. Following, we will focus on the inter-annual and spatiotemporal variability of the phytoplankton phenology in the northern part of the basin.

3.3. Inter-Annual Spatiotemporal Variability in the Northern Red Sea (Bio-Regions 3 and 4)

In order to study the inter-annual variability in the spatial distribution of Bio-regions 3 and 4, an annual clustering method was used and provided 21 annual maps, from 1998 to 2018, (Figure 6). Each map was associated with mean annual cycles of CHL for the two bio-regions considered (Figure 7, black lines). When averaged, the resulting map (Figure 6, right panel) and annual cycles (Figure 7, colored lines) were similar to the ones obtained previously (Figure 1). This suggests that, for the northern Red Sea, the climatological clustering results (Figure 1) described the average state of this basin in term of phytoplankton phenology. In other terms, those previously obtained results (Figure 1) were not the consequences of how the climatological dataset was built.

Over the 21 years, the Bio-region 3 mainly covered the northwestern area of the Red Sea, the Gulf of Aqaba and some parts of the north central Red Sea (20°–23°N). In detail, the Bio-region 3 covered ~46% of the

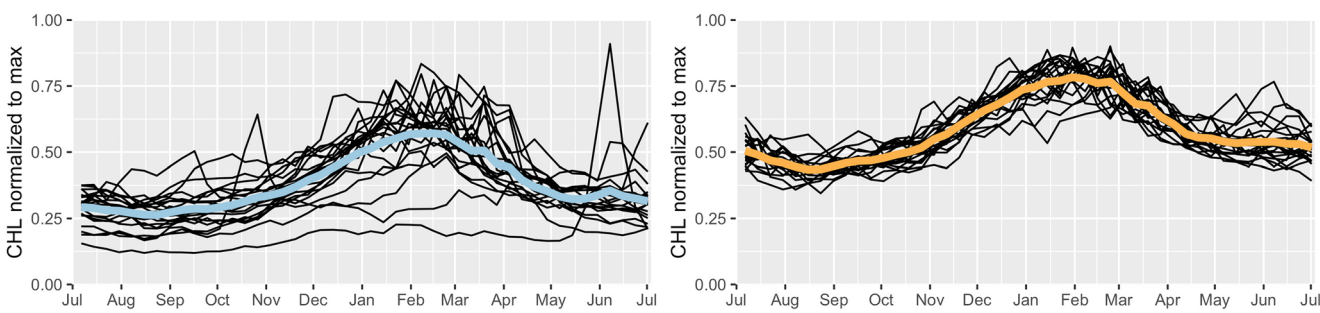

Figure 7. Annual clustering results for the northern half Red Sea (above 20°N). The average annual cycles of normalized chlorophyll-a concentration (thick lines) with all annual cycles (thin lines) for bio-regions #3 and #4.

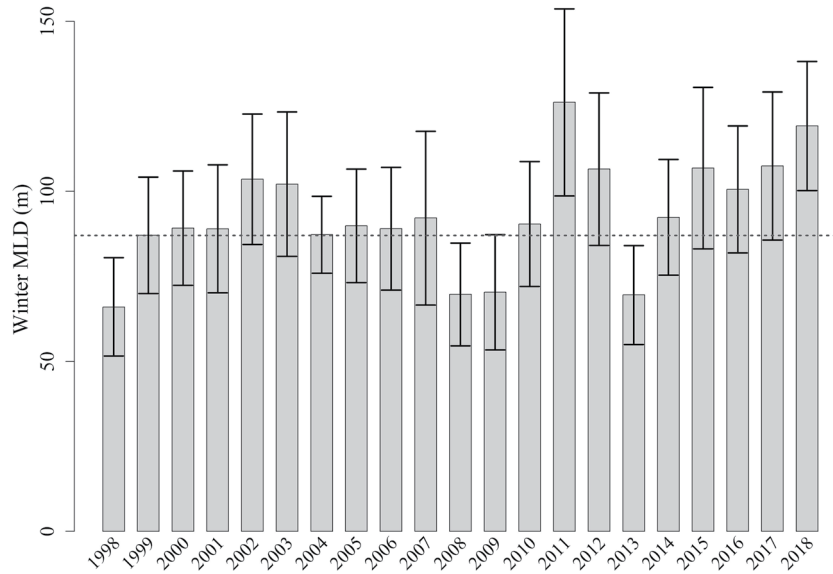

Figure 8. Average ± standard deviation of the winter Mixed Layer Depth within the northwestern Red Sea from 1998 to 2018. The dashed dark gray line represent the average value of the MLD.

northern Red Sea above 25°N, ~29% from 25° to 22.5°N and ~60% from 22° to 20°N (Figure 6). Some annual exceptions were observed in 1998, 2008, 2009 and 2013, during which the northern Red Sea was mainly covered by the Bio-region 4 (Figure 6).

The yearly normalized and non-normalized annual cycles of CHL from 1998 to 2018 also revealed that the Bio-region 3 was characterized by higher inter-annual variability in the phytoplankton phenology (i.e., initiation, duration and termination of the bloom) than Bio-region 4 (Figure 7). Such inter-annual variability could be due to variations in sea surface temperature, surface circulation and/or in mesoscale activity that could modulate the phytoplankton phenology (Dasari et al., 2018; Gittings et al., 2018; Raitsos et al., 2013).

The phytoplankton bloom observed in the northern half of the Red Sea (mostly in Bio-region 3) only occurs when the mixing is deep enough to supply surface layers with nutrients from deep waters (Figure 3) (Gittings et al., 2018 and references therein; Torfstein & Kienast, 2018). Gittings et al. (2018) showed that warmer (colder) conditions might induce a shallower (deeper) MLD due to variations in air-sea heat fluxes, which could control the phytoplankton phenology in this region. This is consistent with some observed inter-annual variations in the spatial distribution of Bio-regions 3 and 4 in the northern area of the Red Sea. As mentioned before, the northern area, normally covered by Bio-region 3 (Figures 1a and 6, right), was mainly covered by Bio-region 4 during the years 1998, 2008, 2009 and 2013 (Figure 6), when the winter MLD in the north-western Red Sea was shallower compare to the average observed value (Figure 8). In contrast, the deepest winter MLD in this area was observed in 2011 (Figure 8), when the northern region was fully covered by Bio-region 3 (Figure 6). This is consistent with Karnauskas and Jones (2018) where they showed that the winter of the year 2011 was an anomalously cool period in the northern Red Sea.

The observed winter bloom in the central part of the Red Sea (dominated by Bio-region 4), seems to be associated with the convergence zone (18°N–25°N) that is formed by opposite surface winds (Figures S3_1, S3_2 and S3_3 in Supporting Information S1, Dasari et al., 2018; Langodan et al., 2014; Raitsos et al., 2013) leading to a zone where nutrients are supplied to the surface waters (Acker et al., 2008). Thus, the position and the intensity of this convergence zone (18°N–25°N), which vary inter-annually due to the ENSO influence (Dasari et al., 2018) might partly explained the inter-annual variability observed (Figures 6 and 7). Indeed, Dasari et al. (2018) showed that the position and the intensity of this convergence zone (18°–25°N) vary inter-annually due to the ENSO influence. Furthermore, note that the observed winter bloom in this region could also result from vertical mixing that dispersed phytoplankton from the deep CHL maximum (Zarokanellos & Jones, 2021).

Furthermore, recent studies showed that other physical processes such as mesoscale features (i.e., eddies and fronts) might supply nutrients within the surface layer in this region, which can stimulate the phytoplankton growth (Asfahani et al., 2020; Kheireddine et al., 2017; Raitsos et al., 2013; Zarokanellos & Jones, 2021). Mesoscale features such as cyclonic and anticyclonic eddies are numerous in this region (Figure S4 in Supporting Information S1) (Zhan et al., 2014, 2018) and favors the transport of nutrients to the surface layers episodically, and thus affect the Red Sea phytoplankton phenology (Kheireddine et al., 2017; Raitsos et al., 2013). The northern Red Sea is also characterized by the recurrent presence of a cyclonic circulation between 25° and 27°N due to the thermohaline circulation as well as wind forces that vary both spatially and temporally (Figures S3 and S4 in Supporting Information S1) (Sofianos & Johns, 2003, 2007). Several studies showed that a such cyclonic circulation induce upwelling of nutrient-rich waters from the deeper layers to the surface layer (Asfahani et al., 2020; Eladawy et al., 2017; Papadopoulos et al., 2013, 2015), which influences the CHL cycle. More physical and biological observations, collected over large areas and during several years, are necessary to assess the importance of such variations in surface winds and circulation in the observed inter-annual changes in phytoplankton phenology.

4. Conclusion

The Red Sea could be divided into four bio-regions with distinct phytoplankton phenology (CHL annual cycles). Their locations and the observed inter-annual variabilities suggested that three main physical mechanisms are likely to influence the phytoplankton phenology in the Red Sea: (a) the fall-winter mixing events in the northern area; (b) the wind convergence zone in the central area and; (c) the monsoon-driven winds in the southern area. In the northern part, winter mixing events due to changes in heat fluxes (Bio-region 3, Figures 1 and 3; Gittings et al., 2018; Papadopoulos et al., 2013, 2015) or associated to the convergence zone (Bio-region 4, Figures 1 and S3_1, S3_2, S3_3 in Supporting Information S1); 18°–25°N, Dasari et al., 2018; Langodan et al., 2014) supplied nutrients at surface that can sustain phytoplankton growth for approximately 5 months. In the southern bio-regions (Bio-regions 1 & 2), which are characterized by a phytoplankton bloom in summer and winter (Figures 1 and 2), the nutrients are supplied through advection of the surface and intermediate waters from the Gulf of Aden in response to the seasonally reversing monsoon winds (Figures S3_1 and S3_3 in Supporting Information S1) (Dreano et al., 2016; Raitsos et al., 2013, 2015; Racault et al., 2015). Only the southern half of the Red Sea is characterized by a summer phytoplankton bloom that generally initiates in June and collapses through August and terminates in September.

Those physical mechanisms, highly variable in response to variations in air-sea heat fluxes and/or ENSO phases, could induce inter-annual variability in phytoplankton phenology patterns observed in the Red Sea. Indeed, the seasonal monsoon winds are highly variable due to changes in ENSO phases, which might explained the high inter-annual variability associated with Bio-regions 1 and 2 and, consequently the inter-annual variations in CHL cycle in the southern half Red Sea. In the northern half of the Red Sea (Bio-regions 3 & 4), the observed inter-annual variations in the CHL annual cycle might be due to year-to-year changes in air-sea heat fluxes, which induce variations in the winter MLD and in the cyclonic circulation (Gittings et al., 2018; Papadopoulos et al., 2013, 2015).

In general, this study shows the potential of using ocean color data to investigate the phytoplankton phenology and reminds the importance of collecting *in situ* measurements in order to have a full understanding about the physical processes that influence the phytoplankton production in the Red Sea. Indeed, ocean color remote sensing data are limited to the surface layer and thus needs to be associated with *in situ* observations. Such high-resolution records of in situ CHL concentrations exist already in the Gulf of Aqaba (Torfstein & Kienast, 2018). Torfstein & Kienast (2018) clearly showed that the winter phytoplankton bloom in the Gulf of Aqaba is associated to a vertical winter mixing that uplift nutrients toward the surface waters in this area (Bio-region 3). Unfortunately, until now, long-term time series of such parameters are still rare in the global ocean (Hawaii Ocean Time-series (HOT, Steinberg et al., 2001), Bermuda Atlantic Time-series Study (BATS, Steinberg et al., 2001) and BOUée pour l'acquiSition d'une Série Optique à Long termE (BOUSSOLE, Antoine et al., 2006). Thanks to the progress in technology, bio-physical interactions along the water column could be studied by using autonomous platforms equipped with biogeochemical sensors (i.e., gliders or profiling floats) which are more and more available in some of the areas of the Red Sea (Asfahani et al., 2020; Kheireddine et al., 2020; Zarokanellos and Jones, 2021). In addition, Gittings, Raitsos

et al. (2019) provided recently the possibility to provide information of phytoplankton size structure in the whole Red Sea from Ocean Colour remote sensing. Thus, it will be possible to investigate on the seasonality, inter-annual variability and phenology of different phytoplankton size classes in relation with their biophysical habitats in future.

Data Availability Statement

The data presented here are freely available by the European Space Agency's Ocean Colour Climate Change Initiative (OC-CCI) (http://www.esa-oceancolour-cci.org), the Copernicus Marine Environment Monitoring Service (CMEMS) Web Portal Subsetter Service and the National Oceanic and Atmospheric Administration (NOAA) (http://www.esrl.noaa.gov/psd/enso/mei/).

Acknowledgments
This study is funded by the King Abdullah University of Science and Technology (KAUST), Kingdom of Saudi Arabia. The authors are grateful to the Ocean Colour CCI team (European Space Agency) for developing, validating and distributing the chlorophyll-a dataset. Computations were done on KAUST's Shaheen II supercomputer. We acknowledge the support of the KAUST Supercomputing Laboratory. We also cordially thanked Adi Torfstein and the other anonymous reviewer for their valuable constructive comments that helped to improve our manuscript.

References

Acker, J., Leptoukh, G., Shen, S., Zhu, T., & Kempler, S. (2008). Remotely-sensed chlorophyll a observations of the northern Red Sea indicate seasonal variability and influence of coastal reefs. *Journal of Marine Systems*, *69*(3–4), 191–204. https://doi.org/10.1016/j.jmarsys.2005.12.006

Antoine, D., Chami, M., Claustre, H., D'Ortenzio, F., Morel, A., Bécu, G., et al. (2006). BOUSSOLE: A joint CNRS-INSU, ESA, CNES and NASA ocean color calibration and validation activity. NASA Technical memorandum N° 2006–214147 (pp. 61). NASA/GSFC.

Ardyna, M., Babin, M., Gosselin, M., Devred, E., Rainville, L., & Tremblay, J. E. (2014). Recent Arctic Ocean sea ice loss triggers novel fall phytoplankton blooms. *Geophysical Research Letters*, *41*(17), 6207–6212. https://doi.org/10.1002/2014gl061047

Ardyna, M., Claustre, H., Sallee, J. B., D'Ovidio, F., Gentili, B., van Dijken, G., et al. (2017). Delineating environmental control of phytoplankton biomass and phenology in the Southern Ocean. *Geophysical Research Letters*, *44*(10), 5016–5024. https://doi.org/10.1002/2016gl072428

Asfahani, K., Krokos, G., Papadopoulos, V. P., Jones, B. H., Sofianos, S., Kheireddine, M., & Hoteit, I. (2020). Capturing a mode of intermediate water formation in the Red Sea. *Journal of Geophysical Research-Oceans*, *125*(4). https://doi.org/10.1029/2019jc015803

Baars, M., Schalk, P., & Veldhuis, M. (1998). Seasonal fluctuations in plankton biomass and productivity in the ecosystems of the Somali Current, Gulf of Aden, and Southern Red Sea. In K. Sherman, E. Okemwa, & M. Ntiba (Eds.), *Large marine ecosystems of the Indian Ocean: Assessment, sustainability, and management* (pp. 394). Blackwell Science, Inc.

Behrenfeld, M. J., & Boss, E. S. (2018). Student's tutorial on bloom hypotheses in the context of phytoplankton annual cycles. *Global Change Biology*, *24*(1), 55–77. https://doi.org/10.1111/gcb.13858

Behrenfeld, M. J., O'Malley, R. T., Siegel, D. A., McClain, C. R., Sarmiento, J. L., Feldman, G. C., et al. (2006). Climate-driven trends in contemporary ocean productivity, *Nature*, *444*. https://doi.org/10.1038/nature05317

Bopp, L., & Le Quéré, C. (2009). Ocean carbon cycle. In C. Le Quéré (Ed.), *Surface ocean—lower atmosphere processes, geophysical monograph series* (Vol. 187, pp. 181–195). American Geophysical Union. https://doi.org/10.1029/2008gm000780

Boyce, D. G., Petrie, B., Frank, K. T., Worm, B., & Leggett, W. C. (2017). Environmental structuring of marine plankton phenology. *Nature Ecology & Evolution*, *1*(10), 1484–1494. https://doi.org/10.1038/s41559-017-0287-3

Boyd, P. W., Claustre, H., Levy, M., Siegel, D. A., & Weber, T. (2019). Multi-faceted particle pumps drive carbon sequestration in the ocean. *Nature*, *568*(7752), 327–335. https://doi.org/10.1038/s41586-019-1098-2

Brewin, R. J. W., Raitsos, D. E., Dall'Olmo, G., Zarokanellos, N., Jackson, T., Racault, M. F., et al. (2015). Regional ocean-color chlorophyll algorithms for the Red Sea. *Remote Sensing of Environment*, *165*, 64–85, https://doi.org/10.1016/j.rse.2015.04.024

Chaidez, V., Dreano, D., Agusti, S., Duarte, C. M., & Hoteit, I. (2017). Decadal trends in Red Sea maximum surface temperature. *Scientific Reports*, *7*. https://doi.org/10.1038/s41598-017-08146-z

Chavez, F. P., Messie, M., & Pennington, J. T. (2011). Marine primary production in relation to climate variability and change. In C. A. Carlson, & S. J. Giovannoni (Eds.), *Marine primary production in relation to climate variability and change*. Annual review of marine science (Vol. 3, pp. 227–260). https://doi.org/10.1146/annurev.marine.010908.163917

Churchill, J. H., Bower, A. S., McCorkle, D. C., & Abualnaja, Y. (2014). The transport of nutrient-rich Indian Ocean water through the Red Sea and into coastal reef systems. *Journal of Marine Research*, *72*(3), 165–181. https://doi.org/10.1357/002224014814901994

Cushing, D. H. (1990). Plankton production and year-class strength in fish populations - An update of the match mismatch hypothesis. *Advances in Marine Biology*, *26*, 249–293. https://doi.org/10.1016/s0065-2881(08)60202-3

Dall'Olmo, G., Dingle, J., Polimene, L., Brewin, R. J. W., & Claustre, H. (2016). Substantial energy input to the mesopelagic ecosystem from the seasonal mixed-layer pump. *Nature Geoscience*, *9*(11), 820–823. https://doi.org/10.1038/ngeo2818

Dasari, H. P., Langodan, S., Viswanadhapalli, Y., Vadlamudi, B. R., Papadopoulos, V. P., & Hoteit, I. (2018). ENSO influence on the interannual variability of the Red Sea convergence zone and associated rainfall. *International Journal of Climatology*, *38*(2), 761–775. https://doi.org/10.1002/joc.5208

de Boyer Montégut, C., Madec, G., Fischer, A. S., Lazar, A., & Iudicone, D. (2004). Mixed layer depth over the global ocean: An examination of profile data and a profile-based climatology. *Journal of Geophysical Research*, *109*(12), 1–20. https://doi.org/10.1029/2004JC002378

D'Ortenzio, F., Antoine, D., Martinez, E., & d'Alcala, M. R. (2012). Phenological changes of oceanic phytoplankton in the 1980s and 2000s as revealed by remotely sensed ocean-color observations. *Global Biogeochemical Cycles*, *26*. https://doi.org/10.1029/2011gb004269

D'Ortenzio, F., & d'Alcala, M. R. (2009). On the trophic regimes of the Mediterranean Sea: A satellite analysis. *Biogeosciences*, *6*(2), 139–148. https://doi.org/10.5194/bg-6-139-2009

Dreano, D., Raitsos, D. E., Gittings, J., Krokos, G., & Hoteit, I. (2016). The Gulf of Aden intermediate water intrusion regulates the southern Red Sea summer phytoplankton blooms. *PLoS One*, *11*(12), e0168440. https://doi.org/10.1371/journal.pone.0168440

Edwards, M., & Richardson, A. J. (2004). Impact of climate change on marine pelagic phenology and trophic mismatch. *Nature*, *430*(7002), 881–884. https://doi.org/10.1038/nature02808

Eladawy, A., Nadaoka, K., Negm, A., Abdel-Fattah, S., Hanafy, M., & Shaltout, M. (2017). Characterization of the northern Red Sea's oceanic features with remote sensing data and outputs from a global circulation model. *Oceanologia*, *59*(3), 213–237. https://doi.org/10.1016/j.oceano.2017.01.002

Genevier, L. G. C., Jamil, T., Raitsos, D. E., Krokos, G., & Hoteit, I. (2019). Marine heatwaves reveal coral reef zones susceptible to bleaching in the Red Sea. *Global Change Biology*, *25*(7), 2338–2351. https://doi.org/10.1111/gcb.14652

Gittings, J. A., Brewin, R. J. W., Raitsos, D. E., Kheireddine, M., Ouhssain, M., Jones, B. H., et al., (2019). Remotely sensing phytoplankton size structure in the Red Sea. *Remote Sensing of Environment*, *234*, 111387. https://doi.org/10.1016/j.rse.2019.111387

Gittings, J. A., Raitsos, D. E., Kheireddine, M., Racault, M. F., Claustre, H., & Hoteit, I. (2019). Evaluating tropical phytoplankton phenology metrics using contemporary tools. *Scientific Reports*, *9*. https://doi.org/10.1038/s41598-018-37370-4

Gittings, J. A., Raitsos, D. E., Krokos, G., & Hoteit, I. (2018). Impacts of warming on phytoplankton abundance and phenology in a typical tropical marine ecosystem. *Scientific Reports*, *8*. https://doi.org/10.1038/s41598-018-20560-5

Karnauskas, K. B., & Jones, B. H. (2018). The interannual variability of sea surface temperature in the Red Sea from 35 years of satellite and in situ observations. *Journal of Geophysical Research: Oceans*, *123*, 5824–5841. https://doi.org/10.1029/2017JC013320

Kheireddine, M., Dall'Olmo, G., Ouhssain, M., Krokos, G., Claustre, H., Schmechtig, C., et al. (2020). Organic carbon export and loss rates in the Red Sea. *Global Biogeochemical Cycles*, *34*(10). https://doi.org/10.1029/2020gb006650

Kheireddine, M., Ouhssain, M., Claustre, H., Uitz, J., Gentili, B., & Jones, B. H. (2017). Assessing pigment-based phytoplankton community distributions in the Red Sea. *Frontiers in Marine Science*, *4*. https://doi.org/10.3389/fmars.2017.00132

Kheireddine, M., Ouhssain, M., Organelli, E., Bricaud, A., & Jones, B. H. (2018). Light absorption by suspended particles in the Red Sea: Effect of phytoplankton community size structure and pigment composition. *Journal of Geophysical Research-Oceans*, *123*(2), 902–921. https://doi.org/10.1002/2017jc013279

Koeller, P., Fuentes-Yaco, C., Platt, T., Sathyendranath, S., Richards, A., Ouellet, P., et al. (2009). Basin-scale coherence in phenology of shrimps and phytoplankton in the North Atlantic Ocean. *Science*, *324*(5928), 791–793. https://doi.org/10.1126/science.1170987

Labiosa, R. G., Arigo, K. R., Genin, A., Monismith, S. G., & Dijken, G. (2003). The interplay between upwelling and deep convective mixing in determining the seasonal phytoplankton dynamics in the gulf of Aqaba: Evidence from SeaWiFS and MODIS. *Limnology & Oceanography*, *48*, 2355–2368. https://doi.org/10.4319/lo.2003.48.6.2355

Lacour, L., Claustre, H., Prieur, L., & D'Ortenzio, F. (2015). Phytoplankton biomass cycles in the North Atlantic subpolar gyre: A similar mechanism for two different blooms in the Labrador Sea. *Geophysical Research Letters*, *42*(13), 5403–5410. https://doi.org/10.1002/2015gl064540

Langodan, S., Cavaleri, L., Viswanadhapalli, Y., & Hoteit, I. (2014). The Red Sea: A natural laboratory for wind and wave modeling. *Journal of Physical Oceanography*, *44*(12), 3139–3159. https://doi.org/10.1175/jpo-d-13-0242.1

Lindel, D., & Post, A. (1995). Ultraphytoplankton succession is triggered by deep winter mixing in the Gulf of Aqaba (Eilat), Red Sea. *Limnology & Oceanography*, *40*(6), 1130–1141. https://doi.org/10.4319/lo.1995.40.6.1130

Martinez, E., Antoine, D., D'Ortenzio, F., & Gentili, B. (2009). Climate-Driven Basin-Scale decadal oscillations of oceanic phytoplankton. *Science*, *326*(5957), 1253–1256. https://doi.org/10.1126/science.1177012

Mayot, N., D'Ortenzio, F., d'Alcala, M. R., Lavigne, H., & Claustre, H. (2016). Interannual variability of the Mediterranean trophic regimes from ocean color satellites. *Biogeosciences*, *13*(6), 1901–1917. https://doi.org/10.5194/bg-13-1901-2016

Morcos, S. A. (1970). Physical and chemical oceanography of the Red Sea. *Oceanography and Marine Biology: An Annual Review*, *8*, 73–202.

Papadopoulos, V. P., Abualnaja, Y., Josey, S. A., Bower, A., Raitsos, D. E., Kontoyiannis, H., et al. (2013). Atmospheric forcing of the winter air-sea heat fluxes over the Northern Red Sea. *Journal of Climate*, *26*(5), 1685–1701. https://doi.org/10.1175/jcli-d-12-00267.1

Papadopoulos, V. P., Zhan, P., Sofianos, S. S., Raitsos, D. E., Qurban, M., Abualnaja, Y., et al. (2015). Factors governing the deep ventilation of the Red Sea. *Journal of Geophysical Research-Oceans*, *120*(11), 7493–7505. https://doi.org/10.1002/2015jc010996

Platt, T., Fuentes-Yaco, C., & Frank, K. T. (2003). Spring algal bloom and larval fish survival. *Nature*, *423*(6938), 398–399. https://doi.org/10.1038/423398b

Racault, M. F., Le Quere, C., Buitenhuis, E., Sathyendranath, S., & Platt, T. (2012). Phytoplankton phenology in the global ocean. *Ecological Indicators*, *14*(1), 152–163. https://doi.org/10.1016/j.ecolind.2011.07.010

Racault, M. F., Raitsos, D. E., Berumen, M. L., Brewin, R. J. W., Platt, T., Sathyendranath, S., et al. (2015). Phytoplankton phenology indices in coral reef ecosystems: Application to ocean-color observations in the Red Sea. *Remote Sensing of Environment*, *160*, 222–234. https://doi.org/10.1016/j.rse.2015.01.019

Racault, M. F., Sathyendranath, S., Brewin, R. J. W., Raitsos, D. E., Jackson, T., & Platt, T. (2017). Impact of El Nino variability on oceanic phytoplankton. *Frontiers in Marine Science*, *4*. https://doi.org/10.3389/fmars.2017.00133

Racault, M. F., Sathyendranath, S., Menon, N., & Platt, T. (2017). Phenological responses to ENSO in the global oceans. *Surveys in Geophysics*, *38*(1), 277–293. https://doi.org/10.1007/s10712-016-9391-1

Racault, M.-F., Sathyendranath, S., & Platt, T. (2014). Impact of missing data on the estimation of ecological indicators from satellite ocean-colour time-series. *Remote Sensing of Environment*, *152*, 15–28. https://doi.org/10.1016/j.rse.2014.05.016

Raitsos, D. E., Pradhan, Y., Brewin, R. J. W., Stenchikov, G., & Hoteit, I. (2013). Remote sensing the phytoplankton seasonal succession of the Red Sea. *PLoS One*, *8*(6), e64909. https://doi.org/10.1371/journal.pone.0064909

Raitsos, D. E., Yi, X., Platt, T., Racault, M. F., Brewin, R. J. W., Pradhan, Y., et al. (2015). Monsoon oscillations regulate fertility of the Red Sea. *Geophysical Research Letters*, *42*(3), 855–862. https://doi.org/10.1002/2014gl062882

Reid, P. C., & Beaugrand, G. (2012). Global synchrony of an accelerating rise in sea surface temperature. *Journal of the Marine Biological Association of the United Kingdom*, *92*(7), 1435–1450. https://doi.org/10.1017/s0025315412000549

Sathyendranath, S., Brewin, R. J. W., Brockmann, C., Brotas, V., Calton, B., Chuprin, A., et al. (2019). An ocean-colour time series for use in climate studies: The experience of the Ocean-Colour climate change initiative (oC-CCI). *Sensors*, *19*, 4285. https://doi.org/10.3390/s19194285

Sathyendranath, S., Jackson, T., Brockmann, C., Brotas, V., Calton, B., Chuprin, A., et al. (2020). ESA ocean colour climate change initiative (Ocean_Colour_cci): Global chlorophyll-a data products gridded on a sinusoidal projection. Version 4.2, Centre for Environmental Data Analysis. Retrieved from https://catalogue.ceda.ac.uk/uuid/99348189bd33459cbd597a58c30d8d10

Sathyendranath, S., Ji, R., & Browman, H. I. (2015). Revisiting Sverdrup's critical depth hypothesis. *ICES Journal of Marine Science*, *72*(6), 1892–1896. https://doi.org/10.1093/icesjms/fsv110

Sofianos, S. S., & Johns, W. E. (2003). An Oceanic General Circulation Model (OGCM) investigation of the Red Sea circulation: 2. Three-dimensional circulation in the Red Sea. *Journal of Geophysical Research-Oceans*, *108*(C3). https://doi.org/10.1029/2001jc001185

Sofianos, S. S., & Johns, W. E. (2007). Observations of the summer Red Sea circulation. *Journal of Geophysical Research*, *112*(C6). https://doi.org/10.1029/2006jc003886

Steinberg, D. K., Carlson, C. A., Bates, N. R., Johnson, R. J., Michaels, A. F., & Knap, A. H. (2001). Overview of the US JGOFS Bermuda Atlantic Time-series Study (BATS): A decade-scale look at ocean biology and biogeochemistry. *Deep-Sea Research Part II: Topical Studies in Oceanography*, *48*, 1405–1447. https://doi.org/10.1016/s0967-0645(00)00148-x

Torfstein, A., & Kienast, S. S. (2018). No correlation between atmospheric dust and surface ocean chlorophyll-a in the oligotrophic Gulf of Aqaba, northern Red Sea. *Journal of Geophysical Research: Biogeosciences*, *123*, 391–405. https://doi.org/10.1002/2017JG004063

Triantafyllou, G., Yao, F., Petihakis, G., Tsiaras, K. P., Raitsos, D. E., & Hoteit, I. (2014). Exploring the Red Sea seasonal ecosystem functioning using a three-dimensional biophysical model. *Journal of Geophysical Research-Oceans*, *119*(3), 1791–1811. https://doi.org/10.1002/2013jc009641

Wolter, K., & Timlin, M. S. (1993). Monitoring ENSO in COADS with a seasonally adjusted principal component index. In *Proceedings of the 17th climate diagnostics workshop*. (pp. 52–57). NOAA/NMC/CAC-NSSL-Oklahoma Climate Survey-CIMMS-School of Meteorology of the University of Oklahoma.

Wolter, K., & Timlin, M. S. (1998). Measuring the strength of ENSO events - How does 1997/98 rank? *Weather*, *53*, 315–324. https://doi.org/10.1002/j.1477-8696.1998.tb06408.x

Wolter, K., & Timlin, M. S. (2011). El Nino/Southern oscillation behaviour since 1871 as diagnosed in an extended multivariate ENSO index (MEI.ext). *International Journal of Climatology*, *31*(7), 1074–1087. https://doi.org/10.1002/joc.2336

Yao, F. C., Hoteit, I., Pratt, L. J., Bower, A. S., Kohl, A., Gopalakrishnan, G., et al. (2014). Seasonal overturning circulation in the Red Sea: 2. Winter circulation. *Journal of Geophysical Research-Oceans*, *119*(4), 2263–2289. https://doi.org/10.1002/2013jc009331

Yao, F. C., Hoteit, I., Pratt, L. J., Bower, A. S., Zhai, P., Kohl, A., & Gopalakrishnan, G. (2014). Seasonal overturning circulation in the Red Sea: 1. Model validation and summer circulation. *Journal of Geophysical Research-Oceans*, *119*(4), 2238–2262. https://doi.org/10.1002/2013jc009004

Zarokanellos, N. D., & Jones, B. H. (2021). Influences of physical and biogeochemical variability of the central Red Sea during winter. *Journal of Geophysical Research: Oceans*, *126*, e2020JC016714. https://doi.org/10.1029/2020JC016714

Zhan, P., Gopalakrishnan, G., Subramanian, A. C., Guo, D. Q., & Hoteit, I. (2018). Sensitivity studies of the Red Sea Eddies using adjoint method. *Journal of Geophysical Research: Oceans*, *123*(11), 8329–8345. https://doi.org/10.1029/2018jc014531

Zhan, P., Subramanian, A. C., Yao, F. C., & Hoteit, I. (2014). Eddies in the Red Sea: A statistical and dynamical study. *Journal of Geophysical Research: Oceans*, *119*(6), 3909–3925. https://doi.org/10.1002/2013jc009563

References From the Supporting Information

Alkawri, A., & Gamoyo, M. (2014). Remote sensing of phytoplankton distribution in the Red Sea and Gulf of Aden. *Acta Oceanologica Sinica*, *33*(9), 93–99. https://doi.org/10.1007/s13131-014-0527-1

Rousseeuw, P. J. (1987). Silhouettes: A graphical aid to the interpretation and validation of cluster analysis. *Journal of computational and applied mathematics*, *20*, 53–65. https://doi.org/10.1016/0377-0427(87)90125-7

Zhan, P., Subramanian, A. C., Yao, F., Kartadikaria, A. R., Guo, D., & Hoteit, I. (2016). The eddy kinetic energy budget in the Red Sea. *Journal of Geophysical Research: Oceans*, *121*, 4732–4747. https://doi.org/10.1002/2015JC011589